Applying a Gene Reversal Rate Computational Methodology to Identify Drugs for a Rare Cancer: Inflammatory Breast Cancer

Cancer Informatics
Volume 22: 1–14

DOI: 10.1177/11769351231202588

Xiaojia Ji, Kevin P Williams and Weifan Zheng

BRITE Institute and Department of Pharmaceutical Sciences, College of Health and Sciences, North Carolina Central University, Durham, NC, USA.

ABSTRACT: The aim of this study was to utilize a computational methodology based on Gene Reversal Rate (GRR) scoring to repurpose existing drugs for a rare and understudied cancer: inflammatory breast cancer (IBC). This method uses IBC-related gene expression signatures (GES) and drug-induced gene expression profiles from the LINCS database to calculate a GRR score for each candidate drug, and is based on the idea that a compound that can counteract gene expression changes of a disease may have potential therapeutic applications for that disease. Genes related to IBC with associated differential expression data (265 up-regulated and 122 down-regulated) were collated from PubMed-indexed publications. Drug-induced gene expression profiles were downloaded from the LINCS database and candidate drugs to treat IBC were predicted using their GRR scores. Thirty-two (32) drug perturbations that could potentially reverse the pre-compiled list of 297 IBC genes were obtained using the LINCS Canvas Browser (LCB) analysis. Binary combinations of the 32 perturbations were assessed computationally to identify combined perturbations with the highest GRR scores, and resulted in 131 combinations with GRR greater than 80%, that reverse up to 264 of the 297 genes in the IBC-GES. The top 35 combinations involve 20 unique individual drug perturbations, and 19 potential drug candidates. A comprehensive literature search confirmed 17 of the 19 known drugs as having either anti-cancer or anti-inflammatory activities. AZD-7545, BMS-754807, and nimesulide target known IBC relevant genes: PDK, Met, and COX, respectively. AG-14361, butalbital, and clobenpropit are known to be functionally relevant in DNA damage, cell cycle, and apoptosis, respectively. These findings support the use of the GRR approach to identify drug candidates and potential combination therapies that could be used to treat rare diseases such as IBC.

KEYWORDS: Gene reversal rate, gene signatures, inflammatory breast cancer, drug repurposing, binary drug perturbation combination

RECEIVED: April 11, 2023. **ACCEPTED:** September 1, 2023.

TYPE: Original Research

FUNDING: The author(s) disclosed receipt of the following financial support for the research, authorship, and/or publication of this article: This work was supported by National Institute of Health grants [U54CA156735, P20CA202924, U54MD012392, R01MD017405, and R15CA223994], with additional support from the Golden LEAF Foundation and the BIOIMPACT Initiative of the State of North Carolina. It was also supported in part by a sub-award from UNC-Chapel Hill to W.Z. from NIH U01CA207160, and from a ROI grant from the UNC System.

DECLARATION OF CONFLICTING INTERESTS: The author(s) declared no potential conflicts of interest with respect to the research, authorship, and/or publication of this article.

CORRESPONDING AUTHORS: Kevin P Williams, BRITE Institute and Department of Pharmaceutical Sciences, College of Health and Sciences, North Carolina Central University, 1801 Fayetteville Street, Durham, NC 27707, USA. Email: kpwilliams@nccu.edu

Weifan Zheng, BRITE Institute and Department of Pharmaceutical Sciences, College of Health and Sciences, North Carolina Central University, 1801 Fayetteville Street, Durham, NC 27707, USA. Email: wzheng@nccu.edu

Introduction

Gene expression reversal methodology is increasingly being utilized to identify potential drugs for repurposing.[1-4] The underlying assumption of these approaches is that a disease can be treated by a drug that has been shown to revert the disease related gene expression signature (GES) back to a normal gene expression state. This approach has been enabled by the fast growth of large publically available gene expression databases such as GEO (Gene Expression Omnibus) at the National Center for Biotechnology Information (NCBI),[5] the large-scale perturbation database termed Connectivity Map (CMap),[6] and the Library of Integrated Network-Based Cellular Signatures (LINCS).[7-9] CMap is a resource that uses cellular responses to perturbations to find relationships between diseases, genes, and therapeutics.[6] The LINCS Center for Transcriptomics at the Broad Institute has generated a more than 1000-fold expansion of CMap.[10] 1.3 million gene expression profiles have been generated by LINCS with L1000 technology, a high-throughput technique to estimate mRNA expression on a genome-wide scale.[10,11] While only ~1000 genes are determined in each L1000 experiment; a model using computational processing of extensive GEO gene expression datasets allows an estimation of the expression of genes (~22 000) in the remaining transcriptome. LINCS L1000 data can be queried using a web-enabled search interface called LINCS Canvas Browser (LCB).[5,12]

Strategies based on gene expression signatures (GES) are advantageous in that they do not require a large amount of a priori knowledge about particular disease targets.[6,13,14] Gene expression data and pharmacologic databases can be combined to detect the gene expression/transcriptome reversal potency of drug candidates for a specific disease.[15,16] Gene expression profiling of drug response GES can be used to predict responses of drugs to disease. For example, recently, Berthelet et al[17] used computational screening of 90 FDA-approved anti-cancer drugs to identify a new BRCA independent GES that can be used to predict breast cancer sensitivity to cisplatin. Compounds that can reverse the gene expression profile of disease-related genes[18,19] can complement those discovered via traditional target-based discovery methods. The potential of this approach was demonstrated by Chen et al,[19] who showed that the potency of a drug to reverse cancer-associated gene expression changes positively correlates with that drug's efficacy in preclinical models of several cancers, including liver cancer models.[20] Using a

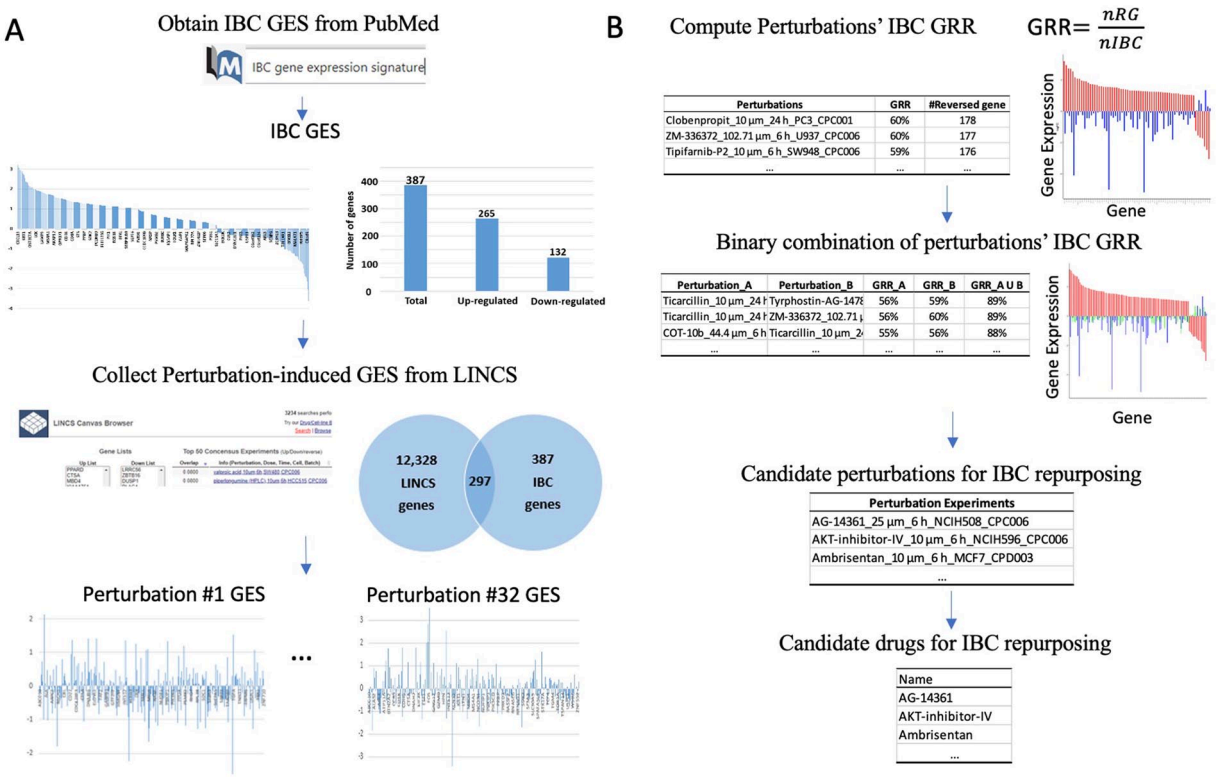

Figure 1. Workflow for using Gene Reversal Rate (GRR) to identify drugs for IBC. Perturbation: Compound under specific experiment conditions such as dose, time-point, and cell-line (from LINCS). (A) Pipeline of IBC and perturbation GESs generation. (B) Pipeline of candidate drugs for IBC repurposing. Abbreviations: GES: gene expression signature; LINCS = Library of integrated network-based cellular signatures.

reverse gene expression scoring (RGES) approach, these authors predicted 4 compounds showing high potency to reverse gene expression in liver cancer,[19] that they further validated as effective in 5 liver cancer cell lines. A number of recent studies have used the gene expression reversal approach to identify drugs for repurposing including for example those for a range of cancers,[21-24] including breast cancer,[25,27] psoriasis,[26] and rare diseases.[27,28]

Inflammatory breast cancer (IBC) is rare, understudied, and the most aggressive subtype of breast cancer.[29-31] IBC represents about 2% to 4% of all diagnosed breast cancers,[32-34] however, it is estimated to account for as high as 8% to 10% of breast cancer deaths in the USA.[14,33,35,36] Compared to non-IBC breast cancer patients, outcomes for IBC patients are worse, such as significantly poor prognosis and survival rate.[37,38] Treatment options for the most aggressive forms of IBC, including triple-negative (TN)-IBC are very limited.[39,40] Recently, common diagnostic criteria to guide treatment and research of IBC was proposed based on clinical, pathologic, and imaging features.[41] New treatment strategies for IBC including genomic profiling are being pursued.[42,43] Several transcriptome-wide gene expression studies have investigated GES for IBC compared to non-IBC.[44] However, the discovery and validation of distinct molecular and/or genetic factors or pathways that are specific for IBC is challenging.[41] An IBC-specific 79-gene expression panel enriched in immune pathways has been identifed,[45] which includes a recently reported subset of adaptive stress response genes.[46] A recent reanalysis of the 79-gene IBC signature identified a prominent role for MYC-mediated transcriptional activity in IBC.[47] In another study, an analysis of TN-IBC and non-TNIBC identified 75 and 81 gene sets that are differentially expressed.[48] There is urgent need to develop therapeutics that target IBC specifically and to identify molecular targets unique to IBC.[30,31]

Here, we aimed to identify drug candidates that have the potential to reverse a GES compiled for IBC. We integrated gene expression patterns for IBC obtained from PubMed publications,[45,48-52] as well as compound/perturbation-induced GESs obtained from open-source datasets (GSE92742) to identify 297 genes related to IBC. With this information, a computational scoring approach termed Gene Reversal Rate (GRR) was implemented to calculate GRRs, and used to identify drug perturbations in the LINCS database that gave the best gene expression reversal potential for IBC. Nineteen (19) drug candidates and 32 drug combinations were identified and are proposed as potential repurposed therapeutics for IBC.

Methods

Overall GRR drug repurposing design

The overall flow of the GRR drug repurposing method is shown in Figure 1. IBC specific GES were obtained from PubMed literature; and perturbation-induced gene expression

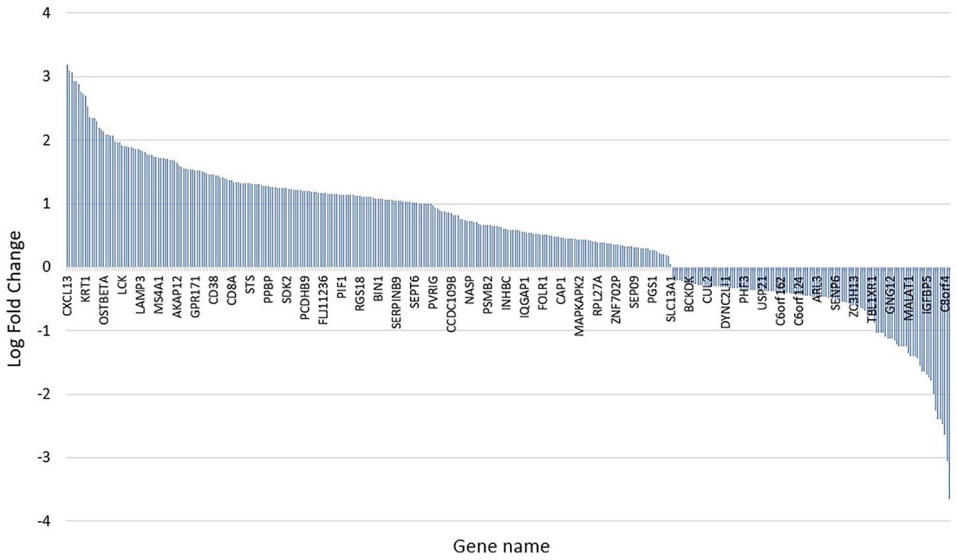

Figure 2. Combined IBC gene expression signature (GES). A total of 387 genes with detailed gene expression data comprise the IBC gene expression signature (265 up-regulated and 122 down-regulated genes). This master IBC-GES (387 genes) was generated from an initial list of 624 IBC-associated genes after removing duplicates and eliminating any genes without associated gene expression log fold change data. The initial 624 genes were collected from 6 PubMed publications.[45,48-52]

profiles collected for each perturbation (drug) candidate from LINCS (https://lincscloud.org/). Once the IBC-GES and perturbation-induced gene expression profiles were obtained, the GRR for each drug perturbation was computed based on the 2 signatures. GRR, based on RGES,[19] was calculated using the number of reversed genes divided by the total number of IBC-specific genes. In addition, the gene expression profiles of binary combinations of the drug perturbations were computed and analyzed against the IBC-specific GES. The GRR of binary combination was calculated using the number of unique reversed genes in both perturbations divided by the total number of IBC-specific genes. This analysis resulted in binary drug combinations as potential "cocktail" treatment options for IBC.

The rationale of our method is based on the idea that a compound or a compound combination that could counteract the gene expression changes of the disease (i.e., IBC in this study) may have beneficial effects against the disease. The scoring scheme should reflect this counteracting effect, and we have adopted the term Gene Reversal Rate (GRR) scoring for this study.

Construction of IBC gene expression signature (GES)

Gene expression data were compiled from prior PubMed publications assessing differential gene expression patterns for IBC.[45,48-52] This gene list was curated to remove duplicates as well as any genes that have no associated gene expression data; and this resulted in the master list of IBC-GES comprising 387 genes with associated gene expression data, including 265 up-regulated and 122 down-regulated genes (see Supplemental Table S1). Figure 2 shows the relative expression profile for all the 387 collated genes in the master IBC-GES.

Perturbation-induced gene expression signatures

Two steps were taken to obtain the perturbation-induced GES to be used for calculating the GRR score against IBC. First, the 387 IBC-related genes compiled above were entered into the LINCS Canvas Browser (LCB) as a query to search against differentially expressed gene lists from the L1000 dataset, which contains ~150 000 experimental conditions (e.g., compounds in different cell lines), to find the top matches.[12] Overlap between the input gene list and the gene lists of each experiment in LINCS are compared by LCB and the top 50 with the highest overlap produced.[12] Experimental conditions were searched that potentially reverse the direction of the gene expression changes of the query (i.e., the IBC gene expression pattern, a gene is reversed from up to down expression or vice versa). The magnitudes of the log fold changes in the datasets are not considered in the matching algorithm.[12] Second, from LINCS (as of Mar 03, 2021, https://lincscloud.org/ hosted by the Connectivity Map Project at the Broad Institute), we downloaded the Level 3 (Q2NORM) gene expression data from a GEO GSE92742 dataset, which consisted of 978 landmark transcripts (L1000 genes) plus inferred genes. This was done using the R package *Slinky* (as of Mar 03, 2021, https://bioconductor.org/packages/release/bioc/html/slinky.html). Gene expression data of the matched experiments were extracted from each of the identified datasets, which were then individually preprocessed using a log2 transformation and normalization approach.

Computation of gene reversal rate scores (GRR) for each perturbation

We define a score termed Gene Reversal Rate (GRR) as the percentage of total IBC-GES genes reversely expressed in a compound perturbation experiment. (i.e., for the IBC gene expression pattern, a gene is reversed from up to down expression or vice versa. The magnitudes of the log fold changes in the datasets are not considered.) The GRRs were computed between the IBC-GES and each of the perturbation's GES. Specifically, for each of the selected perturbations, the GRR was calculated using the number of reversed genes divided by the total number of IBC-specific genes.

$$GRR = \frac{n\text{RG}}{n\text{IBC}} * 100\% \quad (1)$$

where *n*RG = the number of IBC genes reversely expressed in a compound perturbation experiment; *n*IBC = the number of total IBC genes. Here, nIBC = 297.

Binary combination of perturbations

All possible combinations of any 2 perturbations' GES (Gene Expression Signature) were conducted. For each combination of perturbations, a combined GRR was calculated; with those having a high combined GRR selected for further analysis. Note that only the binary (1 or 0) information about whether the genes are up- or down-expressed is used, irrespective of the actual fold values of any expression changes.

Results

Construction of the IBC gene expression signature (GES)

A compiled IBC gene expression list of 624 genes was assembled by us from previously published studies assessing differential gene expression in IBC.[45,48-52] (For more details, see Method and Supplemental Table S1). Figure 2 shows the expression profile for all 387 collated genes in the IBC-GES.

Identification of perturbations that potentially reverse IBC-GES

The 387 IBC-GES was entered into the LINCS Canvas Browser (LCB) as the query to search for matched experiments that could potentially reverse IBC-specific GES. A gene is deemed reversely expressed if expression changes from up to down expression or vice versa. The magnitudes of the log fold changes in the datasets are not considered. The search resulted in a total of 46 matching experiments in LINCS with 32 experiments having associated gene expression data (Table 1).

Perturbation-induced gene expression signatures

Five levels of L1000 data are available for download. Level 3 is the normalized gene expression profiles.[11] Level 3 (Q2NORM) gene expression profiles from the GEO GSE92742 dataset were downloaded (from https://www.ncbi.nlm.nih.gov/geo/query/acc.cgi on March 21, 2021) using R Package Slinky (https://bioconductor.org/packages/release/bioc/html/slinky.html). The gene expression data for the above 32 matched experiments (Table 1) were extracted from each of the identified datasets, which were then individually preprocessed using a log2 transformation and normalization approach. Two hundred ninety-seven of the 387 IBC-GES genes were found to be included in the 12 328 expression genes found in LINCS.

Calculation of Gene Reversal Rate (GRR)

For each of the 32 experiments identified from the LCB search (Table 1), Gene Reversal Rate (GRR) was calculated. The GRR scores ranged from 45% (for ST-209453_10 μm_24 h_PC3_CPC013) to 60% (for ZM-336372_102.71 μm_6 h_U937_CPC006 and Clobenpropit_10 μm_24 h_PC3_CPC001) (Table 2). Figures 3 and 4 show examples of single perturbation drug reversal patterns for drugs Ticarcillin and Tyrphostin-AG-1478, respectfully on the IBC-GES.

Gene expression patterns of binary perturbation combinations

From the 32 selected experiments that have an impact in reversing the IBC-GES (Table 2), we generated all two-way combinations of the perturbation gene expression patterns to give a total of 496 combined expression profiles. Each of these 496 profiles was then compared with the IBC-GES pattern to find the combinations that give the highest gene reversal rates (GRR). The GRR of a single perturbation ranged between 45% and 60% (135-178 genes, Table 2) while the GRR of a binary combination ranged from 50% to 89% (149-264 genes). There are 131 combinations that give a GRR greater than 80%, with 35 of the 131 combinations have a GRR greater than 83%. We chose a threshold of 83% for further analysis. The combination of Ticarcillin_10 μm_24 h_MCF7_CPD003 and Tyrphostin-AG-1478_56.78 μm_6 h_U937_CPC006 had the highest GRR at 89% (Table 3 and Figure 5).

Identification from GRR analysis of drugs that could be repurposed for IBC

From the GRR analysis (Table 3), we identified 20 unique drug perturbations that can potentially be repurposed for IBC (Table 4), which includes 19 individual compounds.

Discussion

We have utilized a computational scoring system, termed Gene Reversal Rate (GRR), to mine public gene expression data sets to identify existing drugs to repurpose for rare and understudied diseases such as IBC. With limited information regarding specific IBC molecular targets, the GRR approach uses only a signature-based scoring function and is based on the RGES

Table 1. Perturbations that potentially reverse IBC-GES.[a]

	INFO (PERTURBATION, DOSE, TIME, CELL, BATCH)[b]
1	Medetomidine_10 µm_6 h_HCC515_CPC005
2	Tipifarnib-P2_10 µm_6 h_SW948_CPC006
3	Tyrphostin-AG-1478_56.78 µm_6 h_U937_CPC006
4	AKT-inhibitor-IV_10 µm_6 h_NCIH596_CPC006
5	AZD-7545_22.2 µm_6 h_NCIH2073_CPC006
6	Clobenpropit_10 µm_24 h_PC3_CPC001
7	Ticarcillin_10 µm_24 h_MCF7_CPD003
8	Ambrisentan_10 µm_6 h_MCF7_CPD003
9	Dapsone_10 µm_24 h_PC3_CPD001
10	BMS-754807_10 µm_6 h_CORL23_CPC006
11	Parthenolide_20 µm_6 h_SNGM_CPC006
12	Tipifarnib_10 µm_6 h_SW948_CPC006
13	Valproic-acid_10 µm_6 h_SW480_CPC006
14	Valproic-acid_10 µm_6 h_SW480_CPD001
15	Butalbital_10 µm_6 h_MCF7_CPD002
16	COT-10b_44.4 µm_6 h_U937_CPC006
17	Piperlongumine_10 µm_6 h_HCC515_CPC006
18	Piperlongumine_10 µm_6 h_SNGM_CPC006
19	ZM-336372_102.71 µm_6 h_U937_CPC006
20	Nicardipine_10 µm_6 h_SKM1_CPC006
21	Ursolic-acid_70.07 µm_6 h_NOMO1_CPC006
22	BMS-536924_11.1 µm_24 h_HT29_CPC006
23	COT-10b_44.4 µm_6 h_SKM1_CPC006
24	Dexamethasone_10 µm_24 h_PC3_CPD001
25	Letrozole_10 µm_24 h_PC3_CPD003
26	Nimesulide_10 µm_6 h_MCF7_CPD001
27	PSH-008_10 µm_24 h_PC3_CPC007
28	AG-14361_25 µm_6 h_NCIH508_CPC006
29	ST-209453_10 µm_24 h_PC3_CPC013
30	Temsirolimus_10 µm_6 h_HT115_CPC006
31	Norepinephrine_10 µm_24 h_MCF7_CPC020
32	TPCA-1_10 µm_6 h_NCIH508_CPC006

[a]LINCS gave a total of 46 matching experiments with 32 experiments having associated gene expression data.
[b]An experiment from LINCS is described in the format of "perturbation, dose, time-point, cell-line, and batch." Experiments that were processed by the L1000 in 1 experimental run are termed a batch. For example, experiment Medetomidine_10 µm_6 h_HCC515_CPC005 means use 10 µm medetomidine treatment for cell line HCC515 for 6 hours in batch CPC005.[12]

Table 2. GRR of perturbations.

PERTURBATIONS[a]	GRR[b] (%)	# REVERSED GENES[c]
Clobenpropit_10 µm_24 h_PC3_CPC001	60	178
ZM-336372_102.71 µm_6 h_U937_CPC006	60	177
Tipifarnib-P2_10 µm_6 h_SW948_CPC006	59	176
Tyrphostin-AG-1478_56.78 µm_6 h_U937_CPC006	59	175
AKT-inhibitor-IV_10 µm_6 h_NCIH596_CPC006	58	171
COT-10b_44.4 µm_6 h_U937_CPC006	57	170
Ambrisentan_10 µm_6 h_MCF7_CPD003	56	167
Ticarcillin_10 µm_24 h_MCF7_CPD003	56	166
Medetomidine_10 µm_6 h_HCC515_CPC005	55	164
COT-10b_44.4 µm_6 h_SKM1_CPC006	55	164
BMS-754807_10 µm_6 h_CORL23_CPC006	55	164
Butalbital_10 µm_6 h_MCF7_CPD002	55	163
AZD-7545_22.2 µm_6 h_NCIH2073_CPC006	54	160
BMS-536924_11.1 µm_24 h_HT29_CPC006	54	160
Letrozole_10 µm_24 h_PC3_CPD003	53	156
Tipifarnib_10 µm_6 h_SW948_CPC006	52	154
Nicardipine_10 µm_6 h_SKM1_CPC006	52	154
Dapsone_10 µm_24 h_PC3_CPD001	52	153
Piperlongumine_10 µm_6 h_SNGM_CPC006	52	153
Temsirolimus_10 µm_6 h_HT115_CPC006	51	151
Nimesulide_10 µm_6 h_MCF7_CPD001	51	150
AG-14361_25 µm_6 h_NCIH508_CPC006	51	150
Valproic-acid_10 µm_6 h_SW480_CPC006	50	149
Valproic-acid_10 µm_6 h_SW480_CPD001	50	149
Parthenolide_20 µm_6 h_SNGM_CPC006	50	148
Piperlongumine_10 µm_6 h_HCC515_CPC006	49	147
Ursolic-acid_70.07 µm_6 h_NOMO1_CPC006	48	142
Norepinephrine_10 µm_24 h_MCF7_CPC020	47	139
Dexamethasone_10 µm_24 h_PC3_CPD001	46	138
PSH-008_10 µm_24 h_PC3_CPC007	46	137
TPCA-1_10 µm_6 h_NCIH508_CPC006	46	136
ST-209453_10 µm_24 h_PC3_CPC013	45	135

[a]An experiment in LINCS is described in the format of "perturbation, dose, time-point, cell-line, and batch." Experiments that were processed by the L1000 in 1 experimental run are termed a batch. For example, experiment Medetomidine_10 µm_6 h_HCC515_CPC005 means use 10 µm Medetomidine was used to treat the cell line HCC515 for 6 hours in batch CPC005.[12]
[b]The Gene Reverse Rate is defined as the percentage of total IBC GES reversely expressed in a compound perturbation experiment and was calculated using the number of reversed genes divided by the total number of IBC-specific genes.
[c]# Reversed gene: number of IBC genes whose expression was reversed in a compound perturbation experiment. A gene is deemed reversely expressed if expression changes from up to down expression or vice versa. The magnitudes of the log fold changes in the datasets are not considered.

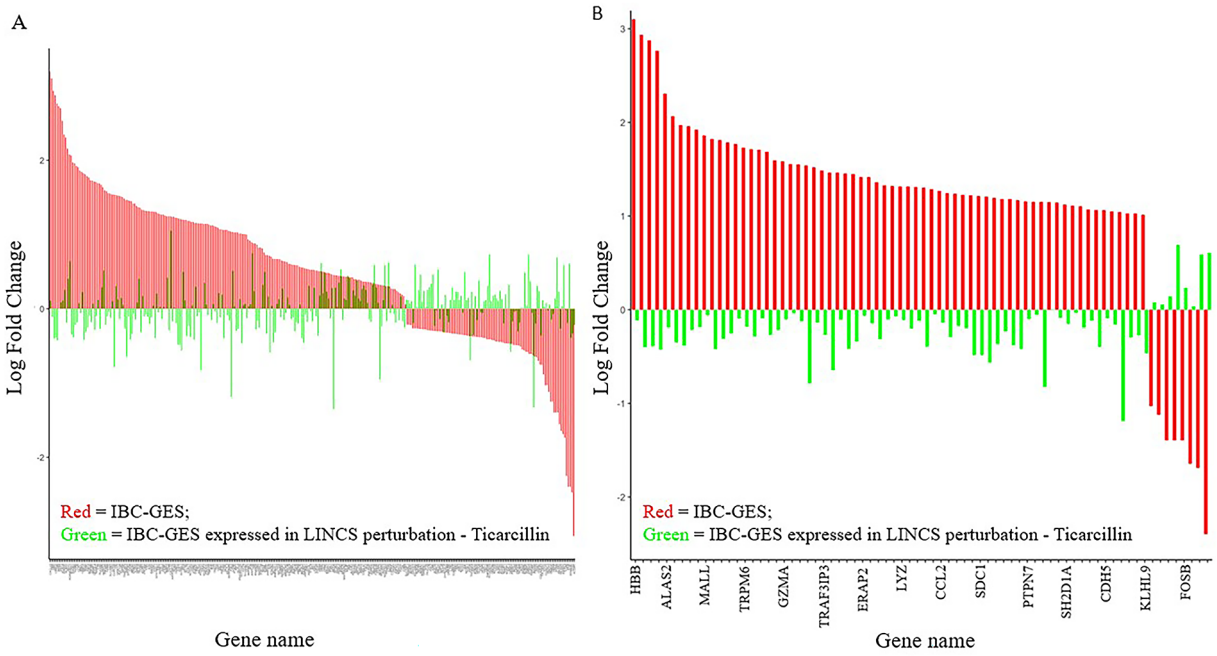

Figure 3. Gene expression patterns for single perturbation Ticarcillin_10 μm_24 h_MCF7_CPD003: (A) overall view of all of the 297 IBC-GES genes expressed in Ticarcillin_10 μm_24 h_MCF7_CPD003 with 56% gene reversal rate (GRR) and (B) focused view of 74 IBC-GES genes (| Log FC | >1, 66 up-regulated, 8 down-regulated) that are reversely expressed in Ticarcillin_10 μm_24 h_MCF7_CPD003.

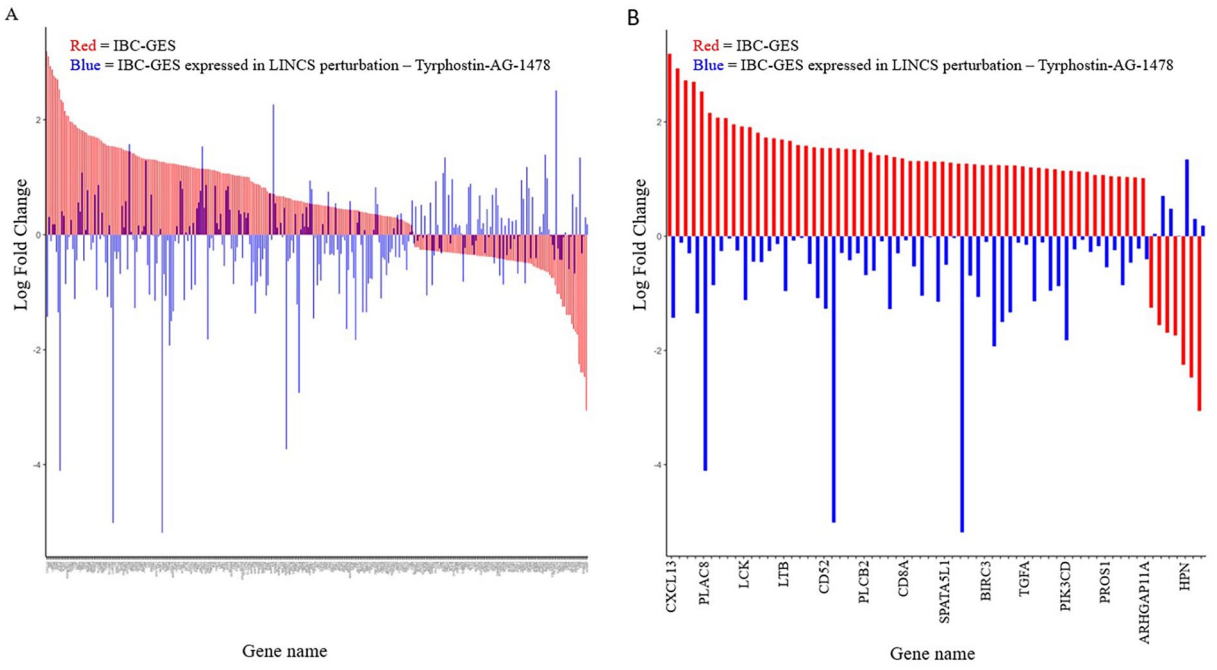

Figure 4. Gene expression patterns for single perturbation Tyrphostin-AG-1478_56.78 μm_6 h_U937_CPC006: (A) overall view of all of the 297 IBC-GES genes expressed in Tyrphostin-AG-1478_56.78 μm_6 h_U937_CPC006 with 59% gene reversal rate (GRR) and (B) focused view of 67 IBC-GES genes (| Log FC | >1, 60 up-regulated, 7 down-regulated) reversely expressed in Tyrphostin-AG-1478_56.78 μm_6 h_U937_CPC006.

approach developed by Chen et al.[19] For our study, first, an IBC gene expression set consisting of 387 genes was collated from published studies.[45,48-52] Two hundred ninety-seven of these 387 IBC-GES genes were identified to be included in the 12 328 expression genes in LINCS. We then used these IBC-associated differentially expressed genes as the query against drug signatures from LINCS. We found that our GRR analysis, in addition to identifying individual compounds/perturbations, also identified binary perturbation combinations of 32 selected experiments with high GRR. Of the 297 genes, 45% to 60% of the genes were reversed by identified single perturbations and 50% to 89% of the genes were reversed by identified binary

Table 3. Binary drug perturbation combinations with GRR ⩾ 83%.

DRUG A[a]	DRUG B[a]	# REVERSED GENES A	GRR A (%)	# REVERSED GENES B	GRR B (%)	# REVERSED GENES A ∪ B[b]	GRR A ∪ B (%)
Ticarcillin	Tyrphostin	166	56	175	59	264	89
Ticarcillin	ZM-336372	166	56	177	60	263	89
COT-10b	Ticarcillin	164	55	166	56	261	88
AZD-7545	Medetomidine	160	54	164	55	254	86
Lobenpropit	Tipifarnib-P2	178	60	176	59	253	85
Letrozole	Ticarcillin	156	53	166	56	253	85
Ambrisentan	ZM-336372	167	56	177	60	251	85
AG-14361	Ticarcillin	150	51	166	56	250	84
AKT-inhibitor-IV	Ambrisentan	171	58	167	56	250	84
AZD-7545	Tipifarnib-P2	160	54	176	59	250	84
Clobenpropit	Ticarcillin	178	60	166	56	250	84
COT-10b	Dapsone	164	55	153	52	250	84
AZD-7545	Clobenpropit	160	54	178	60	249	84
COT-10b	Ticarcillin	170	57	166	56	249	84
COT-10b	Tipifarnib-P2	170	57	176	59	249	84
Temsirolimus	Ticarcillin	151	51	166	56	249	84
Butalbital	ZM-336372	163	55	177	60	248	84
Ambrisentan	COT-10b	167	56	170	57	247	83
Ambrisentan	Tipifarnib-P2	167	56	176	59	247	83
AZD-7545	Ticarcillin	160	54	166	56	247	83
BMS-536924	Medetomidine	160	54	164	55	247	83
BMS-536924	Ticarcillin	160	54	166	56	247	83
BMS-754807	Tipifarnib-P2	164	55	176	59	247	83
Butalbital	COT-10b	163	55	164	55	247	83
Butalbital	COT-10b	163	55	170	57	247	83
COT-10b	Nimesulide	164	55	150	51	247	83
AKT-inhibitor-IV	Clobenpropit	171	58	178	60	246	83
BMS-536924	Tipifarnib-P2	160	58	176	60	246	83
BMS-754807	COT-10b	164	55	164	55	246	83
Clobenpropit	COT-10b	178	60	170	57	246	83
Clobenpropit	ZM-336372	178	60	177	60	246	83
COT-10b	Tipifarnib	164	55	154	52	246	83
COT-10b	Nicardipine	170	57	154	52	246	83
Nicardipine	ZM-336372	154	52	177	60	246	83
Tipifarnib-P2	Tyrphostin	176	59	175	59	246	83

[a]Drug name for each identified perturbation: Compound under specific experiment conditions such as dose, time-point, and cell-line. An experiment is described in the format of "perturbation, dose, time-point, cell-line, and batch."
[b]∪ indicates combination.

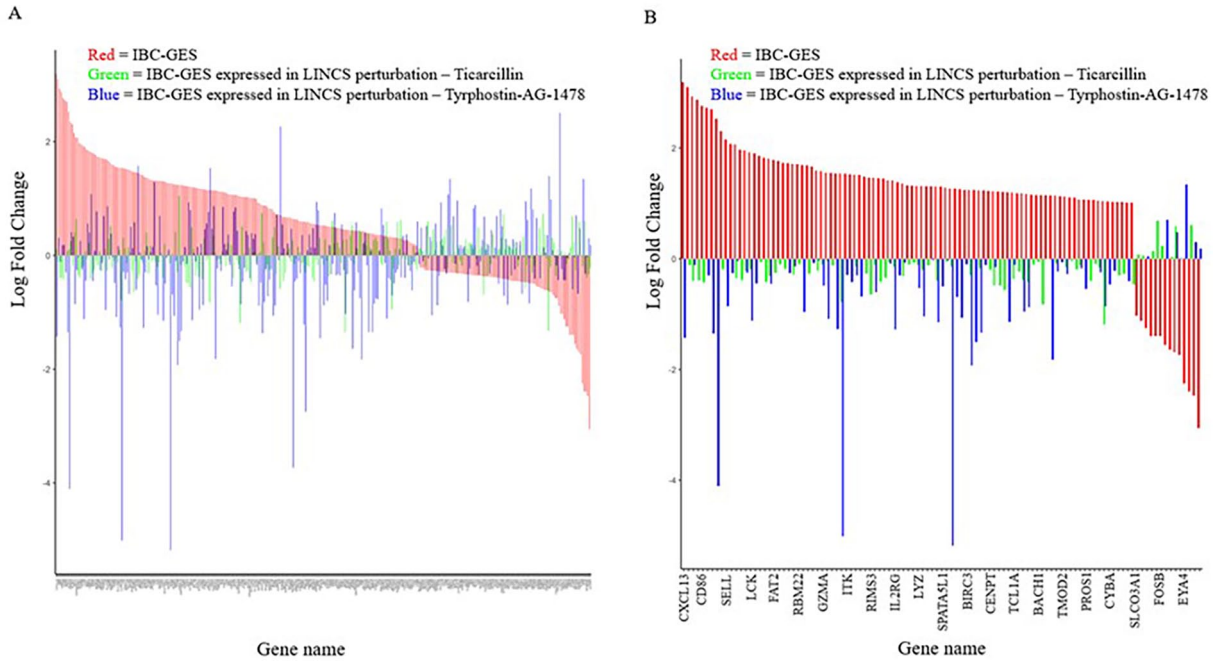

Figure 5. Gene expression patterns of binary combination of Ticarcillin_10 µm_24 h_MCF7_CPD003 and Tyrphostin-AG-1478_56.78 µm_6 h_U937_CPC006: (A) overall view of the 297 IBC-GES genes expressed in binary combination of Ticarcillin_10 µm_24 h_MCF7_CPD003 and Tyrphostin-AG-1478_56.78 µm_6 h_U937_CPC006 with 89% GRR and (B) 109 IBC-GES genes (| Log FC | >1, 95 up-regulated, 14 down-regulated) reversely expressed in binary combination of Ticarcillin_10 µm_24 h_MCF7_CPD003 and Tyrphostin-AG-1478_56.78 µm_6 h_U937_CPC006.

perturbation combinations. From the top 35 binary combinations (GRR greater than 83%), we identified 20 unique perturbations comprising 19 individual drugs that reverse to some degree up to 264 of the 297 genes. These included the following compounds: AG-14361, AKT-inhibitor-IV, Ambrisentan, AZD-7545, BMS-536924, BMS-754807, Butalbital, Clobenpropit, COT-10b, Dapsone, Letrozole, Medetomidine, Nicardipine, Nimesulide, Temsirolimus, Ticarcillin, Tipifarnib-P2, Tyrphostin-AG-1478, ZM-336372. The mechanisms of action (MOA) of these drugs and relevance as potential therapeutics for IBC are discussed below.

Mechanisms of the individual perturbations

Among the 19 compounds identified from our GRR study on IBC, 17 have published findings indicating that they may have potential pharmacologic effects against human cancers with varied mechanisms, spanning anti-proliferation, anti-inflammation, tumor growth reduction, cancer drug resistance, and anti-metastatic potential (Table 5). For example, AG14361, Ambrisentan, AZD7545, and Clobenpropit have been used as anti-cancer therapy for many cancers including breast cancer.[53-58] Anti-cancer agents AKT-inhibitor-IV and BMS-754807 have been shown to have anti-proliferative activities against human cancer cells.[59,60] BMS-536924, Tyrphostin AG-1478, and ZM-336372 significantly suppressed cancer viability, migration, and invasion of different human cancer cells.[61-66] COT-10b, Dapsone, Nicardipine, and Nimesulide are anti-inflammatory drugs and also potential anticancer agents.[67-72] Letrozole has been used in hormone therapy for breast cancer and polycystic ovary syndrome.[73,74] Temsirolimus, a FDA-approved anti-cancer drug has efficacy in certain solid tumors as an inhibitor of angiogenesis.[75] Ticarcillin is active against resistant organisms that commonly affect patients with cancer,[76] and Tipifarnib effectively inhibits tumorigenesis in thyroid cancer.[77] Six of the compounds, Dapsone, Letrozole, Nimesulide, Temsirolimus, Tipifarnib, and Tyrphostin AG-1478, have been studied in various breast cancer models.[73,74,78-83] Rypens et al[47] recently reported that MYC driven expression patterns are overexpressed in IBC. AZD-7545, BMS-754807, and Nimesulide target PDK,[55] Met,[60] and COX[71,72] respectively, which are direct MYC target genes and so these drugs may have relevance for IBC.[47] Al Abo[46] recently reported that adaptive stress response (ASR) genes associated with breast cancer subtypes such as IBC and survival outcomes were functionally relevant in cell cycle, DNA damage response, signal transduction, and regulation of cell death-related processes. AG-14361,[53] butalbital,[84] and clobenpropit[56,57] target DNA damage, cell cycle, and apoptosis respectively, and may be potential therapeutic candidates against IBC. Two of the 19 compounds, Letrozole and Tipifarnib, have different mechanisms of action, and have been tested in clinical trials with varying degrees of success against IBC.[85] Table 5 lists the 19 drugs and their associated mechanisms.

The approval status of the 19 drugs was also investigated (Table 6). Eleven of the 19 predicted compounds: Ambrisentan,

Table 4. LINCS drug perturbations predicted by GRR for IBC.

PERTURBATION EXPERIMENTS
AG-14361_25 μm_6 h_NCIH508_CPC006
AKT-inhibitor-IV_10 μm_6 h_NCIH596_CPC006
Ambrisentan_10 μm_6 h_MCF7_CPD003
AZD-7545_22.2 μm_6 h_NCIH2073_CPC006
BMS-536924_11.1 μm_24 h_HT29_CPC006
BMS-754807_10 μm_6 h_CORL23_CPC006
Butalbital_10 μm_6 h_MCF7_CPD002
Clobenpropit_10 μm_24 h_PC3_CPC001
COT-10b_44.4 μm_6 h_SKM1_CPC006
COT-10b_44.4 μm_6 h_U937_CPC006
Dapsone_10 μm_24 h_PC3_CPD001
Letrozole_10 μm_24 h_PC3_CPD003
Medetomidine_10 μm_6 h_HCC515_CPC005
Nicardipine_10 μm_6 h_SKM1_CPC006
Nimesulide_10 μm_6 h_MCF7_CPD001
Temsirolimus_10 μm_6 h_HT115_CPC006
Ticarcillin_10 μm_24 h_MCF7_CPD003
Tipifarnib-P2_10 μm _6 h_SW948_CPC006
Tyrphostin-AG-1478_56.78 μm_6 h_U937_CPC006
ZM-336372_102.71 μm_6 h_U937_CPC006

An experiment in LINCS is described in the format of "perturbation, dose, time-point, cell-line, and batch." A batch is a collection of experiments that were processed by the L1000 in 1 experimental run. For example, experiment Medetomidine_10 μm_6 h_HCC515_CPC005 means use 10 μm Medetomidine treat cell line HCC515 for 6 hours in batch CPC005.[12] Twelve cell lines are involved in these 20 predicted perturbations in LINCS: 4 large intestine cell lines—NCIH508, HT29, HT115, and SW948; 3 lung cell lines—NCIH596, NCIH2073, and HCC515; 1 breast cancer cell line—MCF7; 1 metastasis: CORL23; 1 prostate—PC3; 1 blood - SKM1; and 1 pleural effusion—U937.

BMS-754807, Butalbital, Dapsone, Letrozole, Medetomidine, Nicardipine, Nimesulide, Temsirolimus, Ticarcillin, and Tipifarnib, are either FDA-approved (https://www.accessdata.fda.gov/scripts/cder/ob/index.cfm) or found in ClinicalTrials (https://www.clinicaltrials.gov/). The remaining 8 compounds, AG-14361, AKT-inhibitor-IV, AZD-7545, BMS-536924, Clobenpropit, COT-10b, Tyrphostin-AG-1478, and ZM-336372, have not been FDA-approved.

Mechanisms of binary combinations of perturbations

Thirty-five (35) of the identified binary perturbation combinations had a GRR greater than 83%. Anti-cancer drug combinations have the potential to enhance therapeutic efficacy compared to a single drug approach as they can target key pathways in a synergistic or additive manner, potentially also reducing drug resistance.[87] In our study, 28 out of the 35 combinations are the results of a binary combination of the 17 compounds with potential activity in cancer mentioned above. For example, the GRR increased from 51% for a single perturbation (such as Temsirolimus and AG14361) to 89% for a binary perturbation combination (such as Ticarcillin + ZM-336372 or Ticarcillin + Tyrphostin AG-1478). The approach to combine therapeutic agents initially used for the treatment of different diseases other than cancer can be effective primarily when the FDA-approved agents target similar pathways to those also found in cancer. In our study, 2 of the 19 compound candidates, Butalbital and Medetomidine, have not to our knowledge, been reported as having anti-cancer activity. Butalbital and Medetomidine, are sedatives that help to decrease anxiety and depression.[84,86] Depression is a common comorbidity in cancer cases where a common biological mechanism may be involved, such as a dysregulated immune system.[88] When Butalbital is combined with COT-10b, Tipifarnib, or ZM-336372, the GRR increased from 55% to 84%. Thus, we propose that Butalbital and Medetomidine may also have potential pharmacologic effects against IBC.

Among these top 35 combinations, the anti-inflammatory drug COT-10b is especially interesting as 12 out of the 35 combinations are a combination with COT-10b (LINCS ID: LSM-6226). COT (Tpl2 in mice) is a serine/threonine MAP3 kinase that regulates production of TNF-a and other pro-inflammatory cytokines such as IL-1b via the ERK/MAP kinase pathway. COT-10b was demonstrated to selectively inhibit the COT pathway following LPS stimulation in macrophages.[67] Since inflammatory signals are a key feature of IBC,[46,89] the identification of COT-10b solely based on its gene expression pattern reversal is significant and needs to be explored. Another interesting drug is Ticarcillin, with 10 of the 35 combinations resulted from a combination of Ticarcillin with other perturbations. Ticarcillin is an antibiotic that is effective against gram-positive cocci and most Gram-negative organisms.[90] Ticarcillin is also active against resistant organisms that commonly affect patients with cancer.[76]

Since 2017, the LINCS database has cataloged ~40 000 unique perturbations from over 50 different human cellular systems using more than 19 000 chemical reagents including drugs and other small molecule chemicals.[10,12] If one conducts a complete binary drug combination of the >19 000 chemical reagents, there would be over 1.8×10^8 possible combinations and it would be impossible to screen all of them by conventional wet-lab high-throughput drug screening approaches. Using the GRR approach, the overall time and costs of identifying combination perturbations can be reduced dramatically, and we quickly identified 35 targeted combinations. Thus, this GRR method can be effective in prioritizing combinations for biological testing. However, the ultimate validation should be based on experimental testing of the combinations predicted by this method. This will be performed in our future work in this area.

Table 5. Mechanisms and molecular targets of GRR identified compounds.

NAME	MECHANISM OF ACTION	TARGET
AG-14361	DNA damage, anti-cancer	PARP1[53,54]
AKT-inhibitor-IV	Cytotoxic and antiproliferative, anti-cancer	Akt[59]
Ambrisentan	Cardiovascular disease	Endothelin Receptor, GPCR & G Protein[58]
AZD-7545	Adenocarcinoma	Pyruvate dehydrogenase kinases (PDK), PDHK[55]
BMS-536924	Suppresses tumor growth	IGF-1R/IR[61]
BMS-754807	Inhibits tumor growth	IGF-1R/InsR, Insulin Receptor, TrkB, Met, TrkA, Aurora A, Aurora B, RON, FLT3[60]
Butalbital	Tension-type headache, cell cycle	Epithelial cell signaling, JAK SATA signaling, P53 signaling, and NOTCH signaling pathway[84]
Clobenpropit	apoptosis, anti-tumor	histamine H3 receptor, PI3K/AKT pathway[56,57]
COT-10b	Acute myeloid leukemia	Serine/threonine MAP3 kinase[67]
Dapsone	leprosy, anti-infection	Immunology/Infection[68]
Letrozole	Cancer	Aromatase[73,74]
Medetomidine	Neurological disease/psychotic disorders	Adrenergic Receptor[86]
Nicardipine	Cardiovascular disease	Calcium Channel[69,70]
Nimesulide	Inflammation	COX, Neuronal Signaling[71,72]
Temsirolimus	Cancer	PI3K/Akt/mTOR[75]
Ticarcillin	Infection	Anti-infection[76]
Tipifarnib	Cancer	farnesyltransferase (FTase)[77]
Tyrphostin-AG-1478	Histiocytic lymphoma	EGFR[62,63]
ZM-336372	Histiocytic lymphoma	JAK/STAT pathway, miR-205, Raf-1[64-66]

A number of complementary signature-based drug screening methodologies have been reported such as machine learning, network analysis, text mining and semantic inference.[3,4,14,91,92] Recently, Yang et al[4] reported a survey of optimal strategies for signature-based drug repositioning, with XSum being identified as the optimal signature matching method for drug retrieval.[93] These analyses[4] also demonstrated that the RGES approach[19,20] was superior to other methods and might serve as an alternative approach. Chen et al[19] developed the RGES approach and applied it to predict and test 4 compounds with efficacy against liver cancer. Shukla et al[2] discussed various signature-based approaches to drug repurposing and suggested an approach for utilizing LINCS resources involving using disease- or phenotype-associated differentially expressed genes (DEG) as the query against the drug signatures. This is consistent with our approach, in that we used an IBC-associated GES as the query against the drug signatures from LINCS. In the literature, the exact sizes of optimal signatures vary substantially, and a query signature size of 100 has been suggested to be applicable for drug retrieval.[4] In our LINCS query, the IBC signature size was 297, which is more than the literature recommended size of 100 and should represent a reasonable reflection of the genetic characteristics of IBC. A caveat to the utility of the gene reversal approach has been suggested recently by Koudijs et al,[15] where they undertook a comprehensive validation of the transcriptome reversion concept and suggest that its potential predictive power may be overstated as many of the drugs identified in these types of studies have general anti-proliferative effects which should be accounted for when trying to identify drugs targeting specific disease relevant pathways. Instead of trying to reverse all differentially expressed genes, a solution suggested by Koudijs et al[15] is to separate upstream driver gene effects from downstream passenger gene effects, which is beyond the scope of our current study.

From our study, 19 compounds are predicted to be potentially useful to be repurposed for treating IBC, with published studies confirming that 17 of the compounds have anti-cancer or anti-inflammatory activities. The 19 compounds we identified by GRR come from different disease areas and have widely varying mechanisms of action, and their potential anti-proliferative effects await experimental verification as part of future studies. An additional beneficial feature of our approach is that we identified drug combinations from different therapeutic

Table 6. FDA-approval status of GRR identified compounds.

NAME	FDA STATUS[a]	CLINICALTRIALS.GOV
AG-14361	Non-approved	No
AKT-inhibitor-IV	Non-approved	No
Ambrisentan	Approved for idiopathic, heritable PAH and connective tissue disease-associated PAH (Pulmonary arterial hypertension.	Yes
AZD-7545	Non-approved	No
BMS-536924	Non-approved	No
BMS-754807	Non-approved	Yes
Butalbital	Approved for headache.	Yes
Clobenpropit	Non-approved	No
COT-10b	Non-approved	No
Dapsone	Approved for inflammatory and infectious diseases.	Yes
Letrozole	Approved for breast cancer and polycystic ovary syndrome (PCOS).	Yes
Medetomidine	Approved for anesthesia.	Yes
Nicardipine	Approved for anti-inflammatory.	Yes
Nimesulide	Approved for anti-inflammatory.	Yes
Temsirolimus	Approved for anticancer drug.	Yes
Ticarcillin	Approved for antibiotic for Gram-negative bacteria.	Yes
Tipifarnib	Non-approved	Yes
Tyrphostin-AG-1478	Non-approved	No
ZM-336372	Non-approved	No

[a]Drug FDA status (for any indication) (https://www.accessdata.fda.gov/scripts/cder/ob/index.cfm) and clinical trials status (https://www.clinicaltrials.gov/) was accessed on 7 July, 2022.

areas; that is, anti-cancer drugs and anti-inflammatory drugs, solely based on the gene expression pattern reversal without any pre-conceived notion of targets and pathways. Our study supports the use of a computational reversal gene expression approach to identify new drug candidates for disease where very few known targets are available. Hence, the GRR approach has potential for identifying new drugs for understudied diseases. In addition, the compounds identified in the present study are not the same as the ones identified in our previous work.[94] The previous paper found 24 molecules based on textual phenotype analysis (i.e., Word2Vec similarity analysis) of cancer-related textual corpus and drugs. The suggested compounds are being evaluated in experimental work ongoing in our laboratory. Our current study has been proposed as a complementary and orthogonal approach to the text mining one. It appears that the gene reversal analysis based on the LINCS database (which contains a much wider set of more than just cancer-related compounds or perturbations) has identified additional different compounds that are not limited to anti-cancer drugs. Even though it would be mutually supporting if both methods identified an overlapping list of compounds, the fact that the 2 lists are not overlapping indicated that the 2 methods are complementary and orthogonal as designed in order to increase the diversity of candidates for drug repurposing.

While we identified a number of novel compounds for potential testing in IBC, challenges in our study include the limited number of IBC cases with associated gene expression data and the development of relevant functional assays to assess the identified drugs for effects in IBC models. Thus, future research should include developing relevant mechanistic functional assays to ensure successful development of these ideas into potential drug candidates for IBC.

Author Contributions

K.P.W. and W.Z. conceived the project. X.J. carried out the study and implemented the methods and analyzed the results. All authors participated in writing the manuscript and approved the final manuscript.

SUPPLEMENTAL MATERIAL

Supplemental material for this article is available online.

REFERENCES

1. Jia Z, Song X, Shi J, et al. Gene signature-based drug repositioning. In: Saxena SK, ed. *Drug Repurposing-Molecular Aspects | Therapeutic Applications* IntechOpen; 2021:283-297.
2. Shukla R, Henkel ND, Alganem K, et al. Signature-based approaches for informed drug repurposing: targeting CNS disorders. *Neuropsychopharmacology*. 2021;46:116-130.
3. Wu H, Huang J, Zhong Y, Huang Q. DrugSig: a resource for computational drug repositioning utilizing gene expression signatures. *PLoS One*. 2017;12:e0177743.
4. Yang C, Zhang H, Chen M, et al. A survey of optimal strategy for signature-based drug repositioning and an application to liver cancer. *eLife*. 2022;11:e71880.
5. Barrett T, Troup DB, Wilhite SE, et al. NCBI GEO: mining tens of millions of expression profiles–database and tools update. *Nucleic Acids Res*. 2007;35:D760-D765.
6. Lamb J, Crawford ED, Peck D, et al. The connectivity map: using gene-expression signatures to connect small molecules, genes, and disease. *Science*. 2006;313:1929-1935.
7. Keenan AB, Jenkins SL, Jagodnik KM, et al. The library of integrated network-based cellular signatures NIH program: system-level cataloging of human cells response to perturbations. *Cell Syst*. 2018;6:13-24.
8. Koleti A, Terryn R, Stathias V, et al. Data portal for the library of integrated network-based cellular signatures (LINCS) program: integrated access to diverse large-scale cellular perturbation response data. *Nucleic Acids Res*. 2018;46:D558-D566.
9. Musa A, Ghoraie LS, Zhang SD, et al. A review of connectivity map and computational approaches in pharmacogenomics. *Brief Bioinform*. 2017;18:903-523.
10. Subramanian A, Narayan R, Corsello SM, et al. A next generation connectivity map: L1000 platform and the first 1,000,000 profiles. *Cell*. 2017;171:1437-1452.e17.
11. Evangelista JE, Clarke DJB, Xie Z, et al. SigCom LINCS: data and metadata search engine for a million gene expression signatures. *Nucleic Acids Res*. 2022;50:W697-W709.
12. Duan Q, Flynn C, Niepel M, et al. LINCS canvas browser: interactive web app to query, browse and interrogate LINCS L1000 gene expression signatures. *Nucleic Acids Res*. 2014;42:W449-W460.
13. Iorio F, Rittman T, Ge H, Menden M, Saez-Rodriguez J. Transcriptional data: a new gateway to drug repositioning? *Drug Discov Today*. 2013;18:350-357.
14. Li J, Zheng S, Chen B, Butte AJ, Swamidass SJ, Lu Z. A survey of current trends in computational drug repositioning. *Brief Bioinform*. 2016;17:2-12.
15. Koudijs KKM, Böhringer S, Guchelaar HJ. Validation of transcriptome signature reversion for drug repurposing in oncology. *Brief Bioinform*. 2023;24:bbac490. doi:10.1093/bib/bbac490
16. He B, Hou F, Ren C, Bing P, Xiao X. A review of current in silico methods for repositioning drugs and chemical compounds. *Front Oncol*. 2021;11:711225.
17. Berthelet J, Foroutan M, Bhuva DD, et al. Computational screening of anti-cancer drugs identifies a new BRCA independent gene expression signature to predict breast cancer sensitivity to cisplatin. *Cancers*. 2022;14:2404. doi:10.3390/cancers14102404
18. van Noort V, Schölch S, Iskar M, et al. Novel drug candidates for the treatment of metastatic colorectal cancer through global inverse gene-expression profiling. *Cancer Res*. 2014;74:5690-5699.
19. Chen B, Ma L, Paik H, et al. Reversal of cancer gene expression correlates with drug efficacy and reveals therapeutic targets. *Nat Commun*. 2017;8:16022.
20. Chen B, Wei W, Ma L, et al. Computational discovery of niclosamide ethanolamine, a repurposed drug candidate that reduces growth of hepatocellular carcinoma cells in vitro and in mice by inhibiting cell division cycle 37 signaling. *Gastroenterology*. 2017;152:2022-2036.
21. Zhao G, Newbury P, Ishi Y, et al. Reversal of cancer gene expression identifies repurposed drugs for diffuse intrinsic pontine glioma. *Acta Neuropathol Commun*. 2022;10:150.
22. Andrade RC, Boroni M, Amazonas MK, Vargas FR. New drug candidates for osteosarcoma: drug repurposing based on gene expression signature. *Comput Biol Med*. 2021;134:104470.
23. Carvalho RF, do Canto LM, Cury SS, Frøstrup Hansen T, Jensen LH, Rogatto SR. Drug repositioning based on the reversal of gene expression signatures identifies TOP2A as a therapeutic target for rectal cancer. *Cancers*. 2021;13:5492. doi:10.3390/cancers13215492
24. Liu LW, Hsieh YY, Yang PM. Bioinformatics data mining repurposes the JAK2 (Janus kinase 2) inhibitor fedratinib for treating pancreatic ductal adenocarcinoma by reversing the KRAS (Kirsten rat sarcoma 2 viral oncogene homolog)-driven gene signature. *J Pers Med*. 2020;10:130. doi:doi: 10.3390/jpm10030130
25. Cui C, Ding X, Wang D, et al. Drug repurposing against breast cancer by integrating drug-exposure expression profiles and drug-drug links based on graph neural network. *Bioinformatics*. 2021;37:2930-2937.
26. Ahmed F, Ho SG, Samantasinghar A, et al. Drug repurposing in psoriasis, performed by reversal of disease-associated gene expression profiles. *Comput Struct Biotechnol J*. 2022;20:6097-6107.
27. Cong Y, Shintani M, Imanari F, Osada N, Endo T. A new approach to drug repurposing with Two-Stage prediction, machine learning, and unsupervised clustering of gene expression. *OMICS*. 2022;26:339-347.
28. Wang Y, Yella JK, Ghandikota S, et al. Pan-transcriptome-based candidate therapeutic discovery for idiopathic pulmonary fibrosis. *Ther Adv Respir Dis*. 2020;14:1753466620971143.
29. Robertson FM, Bondy M, Yang W, et al. Inflammatory breast cancer: the disease, the biology, the treatment. *CA Cancer J Clin*. 2010;60:351-375.
30. Menta A, Fouad TM, Lucci A, et al. Inflammatory breast cancer: what to know about this unique, aggressive breast cancer. *Surg Clin N Am*. 2018;98:787-800.
31. Rosenbluth JM, Overmoyer BA. Inflammatory breast cancer: a separate entity. *Curr Oncol Rep*. 2019;21:86.
32. Chang S, Parker SL, Pham T, Buzdar AU, Hursting SD. Inflammatory breast carcinoma incidence and survival: the surveillance, epidemiology, and end results program of the National Cancer Institute, 1975-1992. *Cancer*. 1998;82:2366-2372.
33. Wang X, Semba T, Phi LTH, et al. Targeting signaling pathways in inflammatory breast cancer. *Cancers*. 2020;12:2479. doi:doi: 10.3390/cancers12092479
34. Lv Q, Liu Y, Huang H, Zhu M, Wu J, Meng D. Identification of potential key genes and pathways for inflammatory breast cancer based on GEO and TCGA databases. *Onco Targets Ther*. 2020;13:5541-5550.
35. Hance KW, Anderson WF, Devesa SS, Young HA, Levine PH. Trends in inflammatory breast carcinoma incidence and survival: the surveillance, epidemiology, and end results program at the National Cancer Institute. *J Natl Cancer Inst*. 2005;97:966-975.
36. Aleksashin NA, Leppik M, Hockenberry AJ, et al. Assembly and functionality of the ribosome with tethered subunits. *Nat Commun*. 2019;10:930.
37. Fouad TM, Barrera AMG, Reuben JM, et al. Inflammatory breast cancer: a proposed conceptual shift in the UICC-AJCC TNM staging system. *Lancet Oncol*. 2017;18:e228-e232.
38. Biswas T, Efird JT, Prasad S, James SE, Walker PR, Zagar TM. Inflammatory TNBC breast cancer: demography and clinical outcome in a large cohort of patients with TNBC. *Clin Breast Cancer*. 2016;16:212-216.
39. Devi GR, Hough H, Barrett N, et al. Perspectives on inflammatory breast cancer (IBC) research, clinical management and community engagement from the Duke IBC consortium. *Cancer*. 2019;10:3344-3351.
40. van Uden DJ, van Laarhoven HW, Westenberg AH, de Wilt JH, Blanken-Peeters CF. Inflammatory breast cancer: an overview. *Crit Rev Oncol Hematol*. 2015;93:116-126.
41. Jagsi R, Mason G, Overmoyer BA, et al. Inflammatory breast cancer defined: proposed common diagnostic criteria to guide treatment and research. *Breast Cancer Res Treat*. 2022;192:245-247.
42. Vagia E, Cristofanilli M. New treatment strategies for the inflammatory breast cancer. *Curr Treat Options Oncol*. 2021;22:50.
43. Lim B, Woodward WA, Wang X, Reuben JM, Ueno NT. Inflammatory breast cancer biology: the tumour microenvironment is key. *Nat Rev Cancer*. 2018;18:485-499.
44. Li X, Kumar S, Harmanci A, et al. Whole-genome sequencing of phenotypically distinct inflammatory breast cancers reveals similar genomic alterations to non-inflammatory breast cancers. *Genome Med*. 2021;13:70.
45. Van Laere SJ, Ueno NT, Finetti P, et al. Uncovering the molecular secrets of inflammatory breast cancer biology: an integrated analysis of three distinct affymetrix gene expression datasets. *Clin Cancer Res*. 2013;19:4685-4696.
46. Al Abo M, Gearhart-Serna L, Van Laere S, et al. Adaptive stress response genes associated with breast cancer subtypes and survival outcomes reveal race-related differences. *NPJ Breast Cancer*. 2022;8:73.
47. Rypens C, Bertucci F, Finetti P, et al. Comparative transcriptional analyses of preclinical models and patient samples reveal MYC and RELA driven expression patterns that define the molecular landscape of IBC. *NPJ Breast Cancer*. 2022;8:12.
48. Funakoshi Y, Wang Y, Semba T, et al. Comparison of molecular profile in triple-negative inflammatory and non-inflammatory breast cancer not of mesenchymal stem-like subtype. *PLoS One*. 2019;14:e0222336.
49. Bertucci F, Ueno NT, Finetti P, et al. Gene expression profiles of inflammatory breast cancer: correlation with response to neoadjuvant chemotherapy and metastasis-free survival. *Ann Oncol*. 2014;25:358-365.
50. Bertucci F, Finetti P, Vermeulen P, et al. Genomic profiling of inflammatory breast cancer: a review. *Breast*. 2014;23:538-545.
51. Woodward WA, Krishnamurthy S, Yamauchi H, et al. Genomic and expression analysis of microdissected inflammatory breast cancer. *Breast Cancer Res Treat*. 2013;138:761-772.
52. Bambhroliya A, Van Wyhe RD, Kumar S, et al. Gene set analysis of post-lactational mammary gland involution gene signatures in inflammatory and triple-negative breast cancer. *PLoS One*. 2018;13:e0192689.

53. Calabrese CR, Almassy R, Barton S, et al. Anticancer chemosensitization and radiosensitization by the novel poly(ADP-ribose) polymerase-1 inhibitor AG14361. *J Natl Cancer Inst*. 2004;96:56-67.
54. Vazquez-Ortiz G, Chisholm C, Xu X, et al. Drug repurposing screen identifies lestaurtinib amplifies the ability of the poly (ADP-ribose) polymerase 1 inhibitor AG14361 to kill breast cancer associated gene-1 mutant and wild type breast cancer cells. *Breast Cancer Res*. 2014;16:R67.
55. Kato M, Li J, Chuang JL, Chuang DT. Distinct structural mechanisms for inhibition of pyruvate dehydrogenase kinase isoforms by AZD7545, dichloroacetate, and radicicol. *Structure*. 2007;15:992-1004.
56. Paik WH, Ryu JK, Jeong KS, et al. Clobenpropit enhances anti-tumor effect of gemcitabine in pancreatic cancer. *World J Gastroenterol*. 2014;20:8545-8557.
57. He W, Yuan QH, Zhou Q. Histamine H3 receptor antagonist clobenpropit protects propofol-induced apoptosis of hippocampal neurons through PI3K/AKT pathway. *Eur Rev Med Pharmacol Sci*. 2018;22:8013-8020.
58. Rivera-Lebron BN, Risbano MG. Ambrisentan: a review of its use in pulmonary arterial hypertension. *Ther Adv Respir Dis*. 2017;11:233-244.
59. Meinig JM, Peterson BR. Anticancer/antiviral agent akt inhibitor-IV massively accumulates in mitochondria and potently disrupts cellular bioenergetics. *ACS Chem Biol*. 2015;10:570-576.
60. Fuentes-Baile M, Ventero MP, Encinar JA, et al. Differential effects of IGF-1R small molecule tyrosine kinase inhibitors BMS-754807 and OSI-906 on human cancer cell lines. *Cancers*. 2020;12:3717. doi:10.3390/cancers12123717
61. Haluska P, Carboni JM, TenEyck C, et al. HER receptor signaling confers resistance to the insulin-like growth factor-I receptor inhibitor, BMS-536924. *Mol Cancer Ther*. 2008;7:2589-2598.
62. Liu Q, Zhang J, Gao H, et al. Role of EGFL7/EGFR-signaling pathway in migration and invasion of growth hormone-producing pituitary adenomas. *Sci China Life Sci*. 2018;61:893-901.
63. Khattab M, Wang F, Clayton AH. UV-vis spectroscopy and solvatochromism of the tyrosine kinase inhibitor AG-1478. *Spectrochim – Mol Biomol Spectrosc*. 2016;164:128-132.
64. Hasegawa T, Adachi R, Iwakata H, Takeno T, Sato K, Sakamaki T. ErbB2 signaling epigenetically suppresses microRNA-205 transcription via Ras/Raf/MEK/ERK pathway in breast cancer. *FEBS Open Bio*. 2017;7:1154-1165.
65. Lohmeyer J, Nerreter T, Dotterweich J, Einsele H, Seggewiss-Bernhardt R. Sorafenib paradoxically activates the RAS/RAF/ERK pathway in polyclonal human NK cells during expansion and thereby enhances effector functions in a dose- and time-dependent manner. *Clin Exp Immunol*. 2018;193:64-72.
66. Blechacz BR, Smoot RL, Bronk SF, Werneburg NW, Sirica AE, Gores GJ. Sorafenib inhibits signal transducer and activator of transcription-3 signaling in cholangiocarcinoma cells by activating the phosphatase shatterproof 2. *Hepatology*. 2009;50:1861-1870.
67. Cusack K, Allen H, Bischoff A, et al. Identification of a selective thieno[2,3-c] pyridine inhibitor of COT kinase and TNF-α production. *Bioorg Med Chem Lett*. 2009;19:1722-1725.
68. Ghaoui N, Hanna E, Abbas O, Kibbi AG, Kurban M. Update on the use of dapsone in dermatology. *Int J Dermatol*. 2020;59:787-795.
69. Chang YY, Jean WH, Lu CW, Shieh JS, Chen ML, Lin TY. Nicardipine inhibits priming of the NLRP3 inflammasome via suppressing LPS-Induced TLR4 expression. *Inflammation*. 2020;43:1375-1386.
70. Hafeez S, Grandhi R. Systematic review of Intrathecal nicardipine for the treatment of cerebral vasospasm in aneurysmal subarachnoid hemorrhage. *Neurocrit Care*. 2019;31:399-405.
71. Chu M, Wang T, Sun A, Chen Y. Nimesulide inhibits proliferation and induces apoptosis of pancreatic cancer cells by enhancing expression of PTEN. *Exp Ther Med*. 2018;16:370-376.
72. Kwon J, Kim S, Yoo H, Lee E. Nimesulide-induced hepatotoxicity: a systematic review and meta-analysis. *PLoS One*. 2019;14:e0209264.
73. Drăgănescu M, Carmocan C. Hormone therapy in breast cancer. *Chirurgia*. 2017;112:413-417.
74. Franik S, Eltrop SM, Kremer JA, Kiesel L, Farquhar C. Aromatase inhibitors (letrozole) for subfertile women with polycystic ovary syndrome. *Cochrane Database Syst Rev*. 2018;5:CD010287.
75. Chen Z, Yang H, Li Z, Xia Q, Nie Y. Temsirolimus as a dual inhibitor of retinoblastoma and angiogenesis via targeting mTOR signalling. *Biochem Biophys Res Commun*. 2019;516:726-732.
76. Fainstein V, Elting L, Pitlik S, Hortobagyi G, Keating M, Bodey GP. Ticarcillin plus clavulanic acid in the treatment of patients with cancer. *Am J Med*. 1985;79:62-66.
77. Untch BR, Dos Anjos V, Garcia-Rendueles MER, et al. Tipifarnib inhibits HRAS-driven dedifferentiated thyroid cancers. *Cancer Res*. 2018;78:4642-4657.
78. Cianchini G, Lembo L, Colonna L, Puddu P. Pemphigus foliaceus induced by radiotherapy and responsive to dapsone. *J Dermatol Treat*. 2006;17:244-246.
79. Güngör T, Ozleyen A, Yılmaz YB, et al. New nimesulide derivatives with amide/sulfonamide moieties: selective COX-2 inhibition and antitumor effects. *Eur J Med Chem*. 2021;221:113566.
80. Banti CN, Papatriantafyllopoulou C, Manoli M, Tasiopoulos AJ, Hadjikakou SK. Nimesulide Silver metallodrugs, containing the mitochondriotropic, triaryl derivatives of pnictogen; anticancer activity against human breast cancer cells. *Inorg Chem*. 2016;55:8681-8696.
81. Jones PR, Butler RD. Spermatozoon ultrastructure of Platichthys flesus. *J Ultrastruct Mol Struct Res*. 1988;98:71-82.
82. Andreopoulou E, Vigoda IS, Valero V, et al. Phase I-II study of the farnesyl transferase inhibitor tipifarnib plus sequential weekly paclitaxel and doxorubicin-cyclophosphamide in HER2/neu-negative inflammatory carcinoma and non-inflammatory estrogen receptor-positive breast carcinoma. *Breast Cancer Res Treat*. 2013;141:429-435.
83. D'Anneo A, Carlisi D, Emanuele S, et al. Parthenolide induces superoxide anion production by stimulating EGF receptor in MDA-MB-231 breast cancer cells. *Int J Oncol*. 2013;43:1895-1900.
84. Silberstein SD, McCrory DC. Butalbital in the treatment of headache: history, pharmacology, and efficacy. *Headache*. 2001;41:953-967.
85. Caceres S, Monsalve B, Alonso-Diez A, et al. Blocking estrogen synthesis leads to different hormonal responses in canine and human triple negative inflammatory breast cancer. *Cancers*. 2021;13:4967. doi:10.3390/cancers13194967
86. Kato K, Itami T, Nomoto K, et al. The anesthetic effects of intramuscular alfaxalone in dogs premedicated with low-dose medetomidine and/or butorphanol. *J Vet Med Sci*. 2021;83:53-61.
87. Bayat Mokhtari R, Homayouni TS, Baluch N, et al. Combination therapy in combating cancer. *Oncotarget*. 2017;8:38022-38043.
88. Sforzini L, Nettis MA, Mondelli V, Pariante CM. Inflammation in cancer and depression: a starring role for the kynurenine pathway. *Psychopharmacology (Berl)*. 2019;236:2997-3011.
89. Rogic A, Pant I, Grumolato L, et al. High endogenous CCL2 expression promotes the aggressive phenotype of human inflammatory breast cancer. *Nat Commun*. 2021;12:6889.
90. Bylund SJEDB. *XPharm: The Comprehensive Pharmacology Reference*. Elsevier; 2007.
91. Bellera CL, Alberca LN, Sbaraglini ML, Talevi A. In silico drug repositioning for chagas disease. *Curr Med Chem*. 2020;27:662-675.
92. Jarada TN, Rokne JG, Alhajj R. A review of computational drug repositioning: strategies, approaches, opportunities, challenges, and directions. *J Cheminform*. 2020;12:46.
93. Cheng J, Yang L, Kumar V, Agarwal P. Systematic evaluation of connectivity map for disease indications. *Genome Med*. 2014;6:540.
94. Ji X, Jin C, Dong X, Dixon MS, Williams KP, Zheng W. Literature-wide association studies (LWAS) for a rare disease: drug repurposing for inflammatory breast cancer. *Molecules*. 2020;25:3933.